

RESEARCH

Open Access



Mapping of stones and their deterioration forms: the Clock Tower, Venice (Italy)

Rebecca Piovesan¹, Elena Tesser¹, Lara Maritan², Gloria Zaccariello¹, Claudio Mazzoli² and Fabrizio Antonelli^{1*}

Abstract

The HYPERION EU project aims to develop a Decision Support System to improve resilience and sustainable reconstruction of historic areas faced with climate change and extreme events. In this context, Venice presents an outstanding example of urban and architectural complexity and richness. The mapping of the ornamental stones of the façade of the Venice Clock Tower (*Torre dell'Orologio*) and their deterioration patterns acts as a milestone on which to build the knowledge-acquisition process of the system as regards stone artefacts and their decay products. The Clock Tower is an early Renaissance building (1499) in Lombardesque style and stands over the entrance to the Mercerie on the northern side of St. Mark's Square. Detailed surveys and mapping of both building materials (mainly stones) and deterioration patterns were carried out, the latter following the glossary of weathering forms, coupled with an easy-to-use scale of evaluation of their intensity. The data output consists of several monothematic maps which can be handled separately, each one focusing on precise lithological or specific deterioration aspects. This study also proposes a simple approach to summarizing the total state of deterioration of the building in the form of a Total Deterioration Rank (TDR) and its representation. The stones used in the façade are regional (*Ammonitico Rosso* and *Scaglia Rossa*) and extra-regional limestones (*Istrian Stone*), as well as Mediterranean white and coloured marbles and stones already used in antiquity (i.e., *Fior di Pesco* or *marmor chalcidicum*, *lapis porphyrites*, a volcanic rock from the Egyptian Eastern Desert, *Proconnesian marble* from the Island of Marmara, *Pavonazzetto toscano* and *white Carrara marble* from the Italian Apuan Alps). The most frequent forms of deterioration detected are black crusts, patinas, discoloration and patterns linked to erosion processes. The interrelation of different mappings led to a number of useful considerations concerning differences in the effectiveness of maintenance procedures between public and private management of the monument.

Keywords *Torre dell'Orologio*, Ancient stones and marbles, Deterioration forms, Weathering, Total Deterioration Rank

Introduction

The Venice Clock Tower (*Torre dell'Orologio*) is an early Renaissance building, designed by Mauro Codussi in the Lombardesque style, which was inaugurated in 1499 [1]. It is located on the northern side of St. Mark's Square

(*Piazza San Marco*) in Venice (north-eastern Italy). It adjoins the eastern end of the *Procuratie Vecchie*, and its lower two floors form a monumental archway into the main street of the city, the *Mercerie*, the economic artery of Venice connecting the religious and political centre (St. Mark's Square) to the commercial and financial area (*Rialto*). The building is composed of a central tower containing the clock, the mechanism of the *Magi*, the statue of the *Madonna*, the sculpture of St. Mark's Lion, and two lower buildings, one on each side, that contain private apartments. The tower is embroidery of blue (blue glass) and gold (copper-based alloy) nestled in a framework of white and grey marbles and Istrian stone (Fig. 1).

*Correspondence:

Fabrizio Antonelli
fabrizio.antonelli@iuav.it

¹ LAMA-Laboratory for the Analysis of Ancient Materials, University Iuav of Venice, Calle della Laca, San Polo 2468, 30125 Venice, Italy

² Department of Geosciences, University of Padova, Via Gradenigo 6, 35131 Padova, Italy



© The Author(s) 2023. **Open Access** This article is licensed under a Creative Commons Attribution 4.0 International License, which permits use, sharing, adaptation, distribution and reproduction in any medium or format, as long as you give appropriate credit to the original author(s) and the source, provide a link to the Creative Commons licence, and indicate if changes were made. The images or other third party material in this article are included in the article's Creative Commons licence, unless indicated otherwise in a credit line to the material. If material is not included in the article's Creative Commons licence and your intended use is not permitted by statutory regulation or exceeds the permitted use, you will need to obtain permission directly from the copyright holder. To view a copy of this licence, visit <http://creativecommons.org/licenses/by/4.0/>. The Creative Commons Public Domain Dedication waiver (<http://creativecommons.org/publicdomain/zero/1.0/>) applies to the data made available in this article, unless otherwise stated in a credit line to the data.

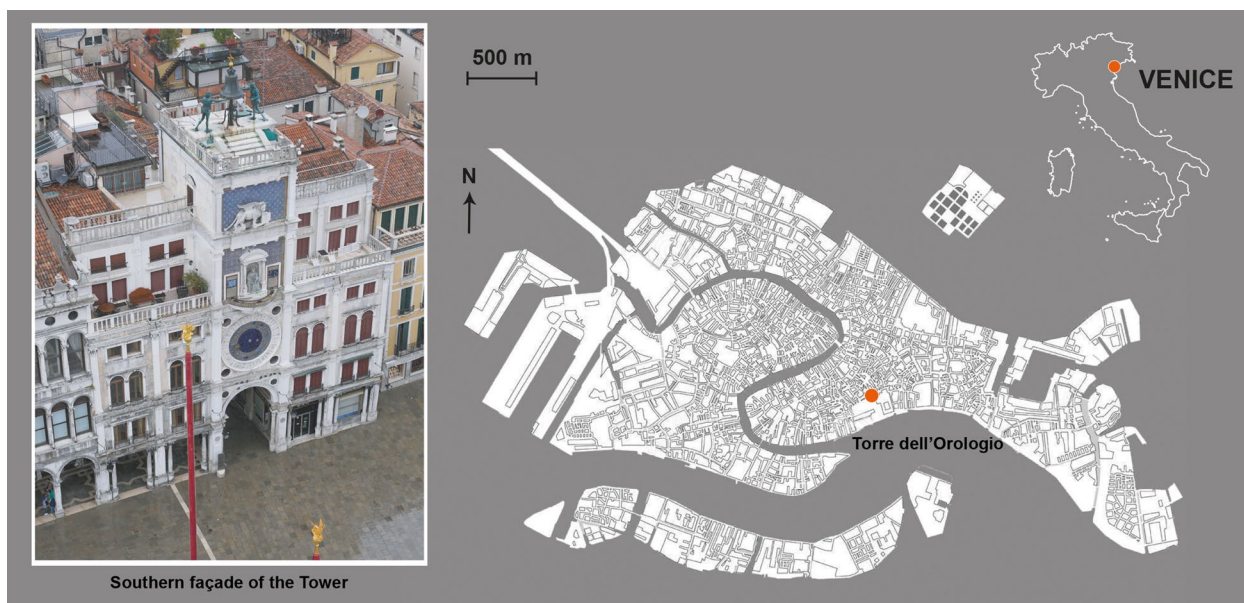


Fig. 1 Geographical location of Venice in Italy and the Clock Tower in Venice. On the left, a picture of the southern façade of the tower

On the top of the tower are the two famous statues of Moors, cast in bronze in 1494 by Ambrosio Delle Anchor, which strike a big bell each hour.

The construction of the Clock Tower took place in three main phases. In 1499, the central part of the building, the actual tower, was completed. A few years later, two side bays were added and finished in the early sixteenth century (1506), conferring an imposing appearance to the building. Finally, in the mid-eighteenth century, the two side bays were crowned with attics to obscure the *Mercurie* houses and eight columns were added to the portico on the ground floor.

From an architectural point of view, the Clock Tower plays a fundamental aesthetic role in St. Mark's Square as a whole and especially in the *Piazzetta* overlooking the Venice lagoon, for which it forms a "theatrical backdrop" of scenographic impact.

To understand the historical and artistic significance of the Clock Tower, however, it has to be considered not only as a building, but also as a scientific installation. Indeed, it was built when Europe was undergoing a scientific and technological revolution in which the measurement of time progressively acquired increasing value, passing from reliable notification (the ringing of bells marking salient moments, such as the beginning and end of the working day) to a continuous and more precise measurement of the passage of time.

Its undisputed architectural and historical importance, and the strategic position of the tower led to the choice of this monument as representative of the city of Venice within the HYPERION EU Project, the presence on the

façades of stones characteristic of the Venetian building tradition constituting an additional point of interest. The main purpose of incorporating this monument into the project as pilot site was to create a baseline from which to start further monitoring of the evolving state of conservation of the artefact.

To this end, precise and in-depth characterisation of the materials and their deterioration products was carried out and mapped in detail. All this information will be made available to the target public (superintendencies, municipalities, restorers and scholars) through the tools of the European project mentioned above.

Mapping is a well-established procedure and the in-situ approach adopted by experts in the field retains its appeal and value [2–7], since the detail achieved by this technique is still not matched by current technologies, although there are several studies that are keen to implement semi-automatic techniques [8–12]. Some works [13, 14] also integrate mere qualitative observation with certain evaluations and indices that allow the intensity and extent of the observed deterioration patterns to be partially quantified. These, although well developed, are sometimes laborious and time-consuming, especially in the case of large buildings decorated with numerous architectural details.

In general, the mapping of deterioration patterns of cultural-heritage building materials remains useful; on the one hand to understand the evolution of the history of art and architecture as well as the choice of materials, and on the other to plan an adequate conservative approach according to the different physical decay and

chemical weathering typologies and on the consequent degree of decay. Moreover, knowledge of the current state of an artefact, with particular attention to the nature and state of conservation of each product used for its preservation over the centuries (an aspect often not featured by written documents) has always been one of the fundamental purposes of cognitive investigations on historical buildings; indeed, this information provides essential guidance for new restoration work [3, 15] and for study of the behaviour of conservation operations in terms of effectiveness and durability. This aspect is particularly important for Venice, where, in the past century, organic and inorganic treatments for stone materials on monumental buildings were widely employed [16–18] often in an experimental way [16, 17, 19]. Therefore, with the aim of classifying and evaluating the materials and deterioration patterns of the Clock Tower, a multi-step survey was carried out on the building. High-resolution orthophotos allowed us to carry out a preliminary recognition of the stones, whereas a detailed on-site survey with the comfort and support of extensive laboratory investigations on selected samples of rocks and deterioration products enabled the construction of thematic maps on an architectural elevation of the building. The methodological approach used here in the on-site mapping, correlated with the indicators used in the specific case of the identification of the degradation level of the artefact (Table 1), is also intended as a suggestion for a more rapid, though still detailed, approach to the recognition of degradation phenomena, their generic distribution and intensity as well as a full assessment of the monument's state of conservation.

Materials and methods

Mapping approach

The mapping procedure was carried out on the southern, western and eastern façades of the Clock Tower. The northern façade was excluded because of its location overlooking the *Mercerie* district, making any investigation and sampling difficult.

The recognition of stones was carried out in three stages: (1) an approximate identification of stone types and their distribution using high-resolution orthophotos; (2) a subsequent detailed in situ investigation; (3) a conclusive characterisation of the uncertain stone materials on the basis of thin-section microscopic mineralogical-petrographic investigations on selected micro-samples.

The identification and classification of the deterioration forms were performed following the indications of the ICOMOS-ISCS glossary [20]. Furthermore, an indicative quantification of the deterioration patterns was carried out with reference to a specifically created table explaining the parameters to be used for the identification of

each type of deterioration form, and the evaluation of the relative degradation level (Table 1). Six damage categories (from 0 to 5, with 0 corresponding to the absence of deterioration and 5 to maximum intensity) were identified as a function of the intensity and extent of each weathering form (Table 1). The evaluation of these parameters was made on a visual comparison basis.

Once the lithological and deterioration patterns had been characterised, a series of thematic maps was produced reporting the distribution of each material and the distribution and intensity of the deterioration forms. The mapping followed several steps: (I) execution of a detailed technical drawing of the building, reporting every single architectural element; (II) production of a preparatory draft of the maps based on the analysis of high-resolution images of the building; (III) on-site survey of the building for the production of detailed maps; (IV) sampling and analysis of the most representative materials and deterioration products; (V) revision of the maps produced on the basis of the laboratory analytical investigations performed on the micro-samples.

To summarise, a specific map was produced for: (I) lithologies; (II) each group of deterioration processes and forms (a total of five maps); (III) Total Deterioration Rank (TDR). The latter is an attempt to produce an overview map which shows the general conservation condition of the building. The TDR value was obtained by taking into account all the deterioration patterns that can be observed contemporaneously on the same elements of the building, and attributing the highest of the values ascribed to the deterioration forms observed (Fig. 2). The legend for each map includes, where necessary and in addition to the colour selection, a series of patterns created specifically for each intensity (Table 1); this proved useful where the overlapping of different deterioration typologies made drawing and reading the map difficult. Small differences (such as the slope of stripes and colour) were provided to the patterns to facilitate distinction of the different subcategories in each thematic map.

Samples

In order to validate and refine the macroscopic recognition, the building materials and their deterioration products were micro-sampled for investigation in the laboratory. In total thirty micro-samples of original stones and decay products were collected from the Clock Tower with the approval of the *Soprintendenza Archeologia, belle arti e paesaggio per il Comune di Venezia e Laguna*. Sampling was carried out following these guidelines:

- A. maximise the variability of rock types and degradation products sampled;

Table 1 Weathering forms identified, reference parameters considered for intensity evaluation, and relative patterns












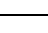

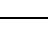





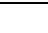
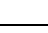

Group of weathering forms	Identified weathering forms	Parameters for intensity evaluation	Deterioration level (DL)	Intensity evaluation	Graphical Pattern
Crack and Deformation	Crack	Width (closed/open), spatial relation to the architectural element (AE) (crossing/not crossing)	1 very slight	Closed, not crossing the AE	
			2 slight	Closed, crossing the AE	
			3 moderate	Open, not crossing the AE	
			4 severe	Open, crossing the AE	
			5 very severe	Open, crossing the AE, dislocation	
	Deformation	Deviation from original shape	1 very slight	Millimetric (mm)	
			2 slight	Centimetric (cm)	
			3 moderate	Decimetric (dm)	
			4 severe	Decimetric (dm), partial dislocation	
			5 very severe	Decimetric (dm), total dislocation	
Detachment	Blistering	Areal extension, lifting height, loss of superficial layer	1 very slight	Centimetric (cm ²) extension, millimetric lifting, no loss of materials	
			2 slight	Centimetric (cm ²) extension, centimetric lifting, no loss of materials	
			3 moderate	Decimetric (dm ²) extension, centimetric lifting, no loss of materials	
			4 severe	Decimetric (dm ²) extension, centimetric lifting, partial loss of superficial layer	
			5 very severe	Decimetric (dm ²) extension, centimetric lifting, abundant loss of superficial layer	
	Disintegration	Areal extension, depth compared with original surface, dusting	1 very slight	From centimetric (cm ²) to decimetric (dm ²) extension, superficial, no evident dusting	
			2 slight	From decimetric (dm ²) to metric (m ²) extension, superficial, no evident dusting	
			3 moderate	From decimetric (dm ²) to metric (m ²) extension, loss of material up to several mm deep, no evident dusting	
			4 severe	From decimetric (dm ²) to metric (m ²) extension, loss of material up to several mm deep, dusting	
			5 very severe	From decimetric (dm ²) to metric (m ²) extension, loss of material up to several cm deep, dusting	
	Peeling	Areal extension, regularity of the peeling area, chromatic contrast	1 very slight	Centimetric (cm ²) isolated areas, no chromatic contrast	
			2 slight	Centimetric (cm ²) isolated areas, chromatic contrast	

Table 1 (continued)















			3 moderate	Decimetric (dm ²) uniform area, no chromatic contrast	
			4 severe	Decimetric (dm ²) uniform area, chromatic contrast	
			5 very severe	Decimetric (dm ²) uniform area, strong chromatic contrast	
Material loss	Erosion	Smoothness, depth compared with original surface	1 very slight	Light polishing of the surface	
			2 slight	Polishing of the surface, loss of material up to several mm deep	
			3 moderate	Light modification of shape (rounding), loss of material up to several mm deep	
			4 severe	Strong modification of shape (rounding), loss of material up to several cm deep only in some areas (differential erosion)	
			5 very severe	Strong modification of shape (rounding), homogeneous loss of material up to several cm deep	
	Microkarst	Areal extension, level of diffusion, depth compared with original surface	1 very slight	Centimetric (cm ²) extension, up to 5 marks for dm ² , superficial	
			2 slight	Decimetric (dm ²) extension, up to 10 marks for dm ² , superficial	
			3 moderate	Decimetric (dm ²) extension, up to 20 marks for dm ² , superficial and deep	
			4 severe	Decimetric (dm ²) extension, up to 30 marks for dm ² , deep	
			5 very severe	Decimetric (dm ²) extension, more than 30 marks for dm ² , very deep	
	Missing Part	Depth and areal extension, aesthetic relevance	1 very slight	Centimetric (cm ²) extension, less than 1 cm deep, no aesthetic relevance	
			2 slight	Centimetric (cm ²) extension, 1 to 5 cm deep, no aesthetic relevance	
			3 moderate	Decimetric (dm ²) extension, 5 to 10 cm deep, low aesthetic relevance	
			4 severe	Decimetric (dm ²) extension, 5 to 10 cm deep, aesthetically damaging	
			5 very severe	Decimetric (dm ²) extension, more than 10 cm deep, severely aesthetically damaging	
Discoloration and deposit	Crust	Darkness, thickness, variability in thickness	1 very slight	White or light grey, homogeneous millimetric (mm) thickness	
			2 slight	Grey or black, homogeneous millimetric (mm) thickness	

Table 1 (continued)








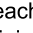
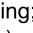






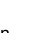

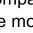
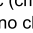
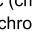
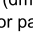
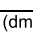


























			3 moderate	White or light grey, not homogeneous millimetric (mm) thickness	
			4 severe	Grey or black, homogeneous centimetric (cm) thickness	
			5 very severe	Grey or black, not homogeneous centimetric (cm) thickness	
	Discoloration (Bleaching; Staining)	Areal extension, chromatic contrast	1 very slight	Centimetric (cm ²) extension, slight chromatic contrast	Bl.  St. 
			2 slight	Decimetric (dm ²) extension, slight chromatic contrast	Bl.  St. 
			3 moderate	Decimetric (dm ²) extension, strong chromatic contrast	Bl.  St. 
			4 severe	Metric (m ²) extension, slight chromatic contrast	Bl.  St. 
			5 very severe	Metric (m ²) extension, strong chromatic contrast	Bl.  St. 
	Efflorescence	Areal extension, morphology, compactness	1 very slight	Decimetric (dm ²) extension, evanescent whisker-like crystals	
			2 slight	Decimetric (dm ²) extension, whisker-like crystals	
			3 moderate	Decimetric (dm ²) extension, powdery deposit	
			4 severe	More than decimetric (> dm ²) extension, compact deposit following the morphology of the substrate	
			5 very severe	More than decimetric (> dm ²) extension, compact deposit deforming the morphology of the substrate	
	Graffiti	Areal extension, chromatic intensity	1 very slight	Centimetric (cm ²) extension, engraved, no chromatic contrast	
			2 slight	Centimetric (cm ²) extension, engraved, chromatic contrast	
3 moderate			Decimetric (dm ²) extension, engraving or painted chromatic contrast		
4 severe			Decimetric (dm ²) extension, engraving or painted strong chromatic contrast		
5 very severe			Metric (m ²) extension, painted, strong chromatic contrast		
Patina	Areal extension, chromatic intensity, homogeneity	1 very slight	Centimetric (cm ²) isolated areas		
		2 slight	Decimetric (dm ²) isolated areas, slightly coloured		
		3 moderate	Decimetric (dm ²) isolated areas, strongly coloured		
		4 severe	Decimetric (dm ²) to metre (m ²) uniform area, slightly coloured		
		5 very severe	Decimetric (dm ²) to metre (m ²) uniform area, strongly coloured		

Table 1 (continued)

	Soiling	Areal extension, chromatic contrast	1 very slight	Centimetric (cm ²) extension, slight chromatic contrast	
			2 slight	Decimetric (dm ²) extension, slight chromatic contrast	
			3 moderate	Decimetric (dm ²) extension, strong chromatic contrast	
			4 severe	Metric (m ²) extension, slight chromatic contrast	
			5 very severe	Metric (m ²) extension, strong chromatic contrast	
Biological colonization	Lichen (and fungus)	Areal extension, growing density, colour intensity	1 very slight	Centimetric (cm ²) extension, sparse growth, light characteristic colour	Li  Fu 
			2 slight	Decimetric (dm ²) extension, sparse growth, light characteristic colour	Li  Fu 
			3 moderate	Decimetric (dm ²) extension, thick growth, moderate characteristic colour	Li  Fu 
			4 severe	Decimetric (dm ²) to metre (m ²) extension, thick growth, moderate characteristic colour	Li  Fu 
			5 very severe	Metre (m ²) extension, thick growth, intense characteristic colour	Li  Fu 
	Moss	Areal extension	1 very slight	Centimetric (cm ²) extension, sparse growth, light characteristic colour	
			2 slight	Decimetric (dm ²) extension, sparse growth, light characteristic colour	
			3 moderate	Decimetric (dm ²) extension, thick growth, moderate characteristic colour	
			4 severe	Decimetric (dm ²) to metre (m ²) extension, thick growth, moderate characteristic colour	
			5 very severe	Metre (m ²) extension, thick growth, intense characteristic colour	

- B. preserve the macroscopic appearance of the sampled element, avoiding damage to sound surfaces;
- C. restrict sampling operations to surfaces already damaged;
- D. choose the sample size according to the needs of the planned analyses.

A list of the samples, their nature, locations on the building, and the analyses performed for each of them is shown in Table 2.

Analytical methods

The collected samples (Table 2) were subjected to petrographic, chemical and biological analyses to classify and characterise them. The analytical methods are summarised below.

Polarized-light optical microscopy (PLOM) and optical microscopy (OM)

The petrographic and textural characteristics of stones were examined through study of standard (30 µm-thick)

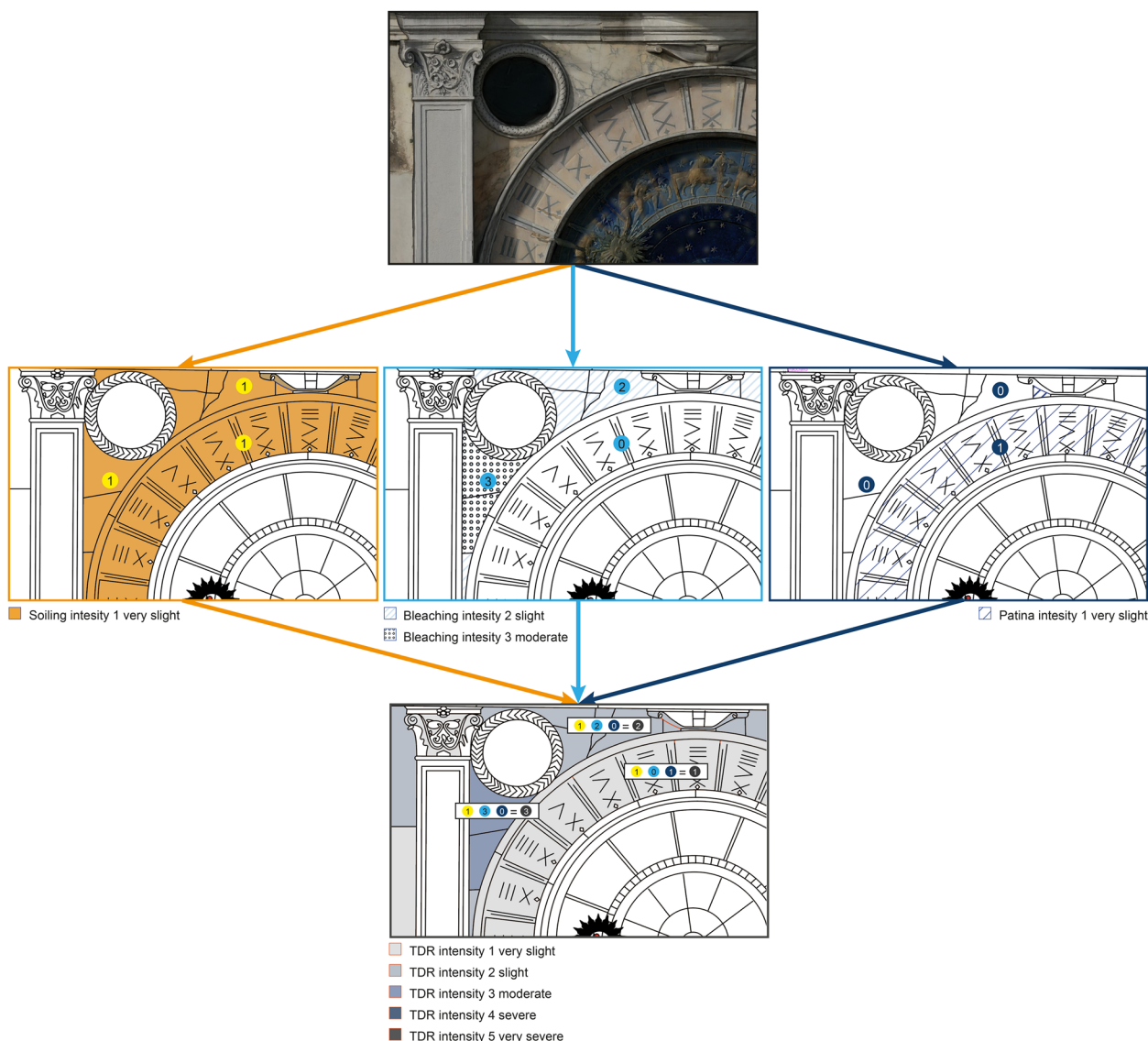


Fig. 2 Illustrative scheme of the procedure followed for the attribution of the TDR

thin sections observed under a polarized-light optical microscope.

Biological colonisations present on the surface of some building stones were observed using an optical microscope. In order to identify the different biodeteriogens, fresh slides were prepared [21]. Histochemical test based on a saturated solution of potassium hydroxide (KOH) was carried out to highlight the presence and facilitate the identification of lichens, according to [22]. The reagent was applied in small quantities to the thallus or apothecia using the needle of a syringe. In the case of a positive reaction (K^+), the part changed colour; otherwise, the reaction has to be considered negative (K^-).

X-Ray powder diffraction (XRPD)

Mineralogical analyses were performed on fine-grained powder samples (obtained with a hand mortar) by X-ray powder diffraction using a Panalytical Empyrean diffractometer, operating at 40 kV and 40 mA, in Bragg–Brentano reflection geometry and equipped with $CuK\alpha$ radiation and an X’Celerator detector. Qualitative analysis of diffraction data was carried out with X’Pert HighScore Plus® software (PANalytical) and the PDF-2 database. The reference intensity ratio (RIR) method, rather than the intensity of the peak channel alone, was used to semi-quantify the amount of the recognized materials in the multiphase XRPD patterns.

Table 2 Location of the samples, materials, and analyses performed on each sample

ID sample	Façade	Material	Sampling location	Analyses
1E	East	Stone	From the stone cladding slab on the north side of the eastern wall. At a height of about 1.00 m from the bottom of the balustrade	PLOM; XRPD; SEM-EDX; IC
2E		Stone	From the crystalline-marble hexagonal cladding slab on the north side of the eastern wall. At a height of about 1.00 m from the bottom of the balustrade	PLOM
3E		Stone	At the beginning of the eastern terrace, from a pillar of the balustrade looking north, near the door. At a height of about 1.00 m from the bottom of the balustrade	PLOM; XRPD; SEM-EDX
5E		Stone	On the eastern terrace, from the capital of a small column of the balustrade looking south. At a height of about 0.70 m from the bottom of the balustrade	PLOM; XRPD; SEM-EDX; IC
6E		Stone + black deposit	From the crystalline-marble hexagonal cladding slab on the south side of the eastern wall. At a height of about 1.60 m from the bottom of the balustrade	OM (Bio); XRPD; μ FTIR
7E		Powder	On the eastern terrace, from a small column of the balustrade looking south. At a height of about 0.50 m from the bottom of the balustrade	XRPD; IC
8E		Powder	On the eastern terrace, from a small column of the balustrade looking south. At a height of about 0.50 m from the bottom of the balustrade	XRPD
9E		Biological deposit	On the eastern terrace, from the top handrail of the balustrade looking south. At a height of about 1.00 m from the bottom of the balustrade	OM (Bio)
10E		Biological deposit	On the eastern terrace, from the top handrail of the balustrade looking south. At a height of about 1.00 m from the bottom of the balustrade	OM (Bio)
11E		Biological deposit	On the eastern terrace, from the top handrail of the balustrade looking south. At a height of about 1.00 m from the bottom of the balustrade	OM (Bio)
12E		Biological material	On the eastern terrace, from the pavement of the balustrade. From the floor	OM (Bio)
1N	North	Stone	On the terrace behind the Moors, from the second step under the statues. At a height of about 1.00 m above the terrace floor	OM (Bio); PLOM; XRPD; IC
2N		Stone + green and black deposits	On the terrace behind the Moors, from the east side of the first step under the statues. At a height of about 1.20 m above the terrace floor	PLOM; XRPD; SEM-EDX; μ FTIR; IC
3N		Stone	On the terrace behind the Moors, from a small column of the balustrade looking north. At a height of about 0.30 m above the terrace floor	PLOM; XRPD
4N		Stone + green deposits	On the terrace behind the Moors, from the west side of the first step under the statues. At a height of about 1.30 m above the terrace floor	PLOM; XRPD; SEM-EDX; IC
1S	South	Stone + yellow patina	On the ground floor, from the eastern column of the central archway of the colonnade facing St. Mark's Square. At a height of about 1.60 m above the square floor	PLOM; XRPD; μ FTIR
2S		Very thin black crust	On the ground floor, from the second pillar of the eastern wing of the colonnade facing St. Mark's Square. At a height of about 1.50 m above the square floor	XRPD; SEM-EDX; IC
3S		Organic patina	On the ground floor, from the third column of the eastern wing of the colonnade facing St. Mark's Square. At a height of about 1.00 m above the square floor, just above the column base	μ FTIR
4S		Black crust	On the ground floor, from the Corinthian capital of the second semi-column of the eastern wing of the colonnade facing St. Mark's Square. At a height of about 3.70 m above the square floor	XRPD; SEM-EDX

Table 2 (continued)

ID sample	Façade	Material	Sampling location	Analyses
5S		Black crust	On the ground floor, from the Corinthian capital of the fourth column of the western wing of the colonnade facing St. Mark's Square. At a height of about 3.70 m above the square floor	XRPD; SEM-EDX; IC
1W	West	Stone + black deposits	On the western terrace, from a stone shelf at the west end of the terrace. At a height of about 1.00 m above the balustrade floor	OM (Bio); PLOM; XRPD; SEM-EDX; IC
2W		Biological deposit	On the western terrace, from the top handrail of the balustrade looking south. At a height of about 1.00 m above the balustrade floor	OM (Bio)
3W		Biological deposit	On the western terrace, from the top handrail of the balustrade looking north. At a height of about 1.00 m above the balustrade floor	OM (Bio)
4W		Yellowish organic patina (powder)	From the crystalline-marble hexagonal cladding slab on the north side of the western wall. At a height of about 1.30 m above the balustrade floor	XRPD; μ FTIR
5W		Stone	On the western terrace, from a small column of the balustrade looking south. At a height of about 0.50 m above the balustrade floor	PLOM; XRPD; SEM-EDX; IC
6W		Black crust	On the western terrace, from the top handrail of the balustrade looking south. At a height of about 1.00 m above the balustrade floor	μ FTIR
7W		Yellowish organic patina (powder)	From the crystalline-marble hexagonal cladding slab on the south side of the western wall. At a height of about 1.30 m above the balustrade floor	XRPD; μ FTIR
8W		Stone	On the western terrace, from the southern side of the doorjamb. At a height of about 1.20 m above the balustrade floor	PLOM; XRPD; SEM-EDX; IC
9W		Stone	On the western wall, from the arch of the doorframe. At a height of about 2.50 m above the balustrade floor	PLOM; XRPD

PLOM polarised light optical microscopy, XRPD X-ray powder diffraction, SEM-EDX scanning electron microscope coupled with energy dispersive X-ray spectrometry, IC chromatography analysis, OM (Bio) biological analysis, μ FTIR Fourier-transform infrared spectroscopy

Scanning electron microscopy and energy dispersive X-ray spectroscopy (SEM-EDX)

Micro-morphological and textural investigations were carried out using a ZEISS EVO15 scanning electron microscope (SEM) equipped with a LaB₆ cathode coupled with an X Flash 6160 BRUKER energy-dispersive X-ray spectroscopy (EDX) system. Samples were prepared as polished thick stratigraphic cross-sections or studied as such after being gold or graphite-coated.

Fourier-transform infrared spectroscopy (μ -FTIR)

Organic compounds identification was performed by means of a ThermoFisher Scientific iN10 Infrared Microscope. A small amount of powder was sampled from the stone surface, using a needle, deposited and pressed on a standard KBr pellet, then analysed in transmittance mode.

Chromatography analysis (IC)

Chemical analyses of the main ions couponing salts were performed by means of a ThermoFisher Scientific

Dionex Aquion Ion Chromatography System. Samples were prepared as fine-grained powder, weighed, dispersed in pure water and the solutions analysed after filtration. Analysing standard solutions enabled the results to be validated.

Results

The stones

Five stones historically used in the Venetian architecture, i.e., two crystalline marbles, (white Carrara marble and Proconnesian marble), and three limestones (*Istrian Stone*, *Ammonitico Rosso* from Verona, and Venetian *Scaglia Rossa*) were identified throughout a correlation of macroscopic and petrographic investigations. A further three well-known lithotypes, i.e., one crystalline marble (*Pavonazzetto Toscano*), one volcanic rock (*Porfido Rosso Antico* or *Lapis Porphyrites*), and a *cataclastic limestone* (*Fior di Pesco*) were identified on the basis of their typical macroscopic characteristics observed *in-situ*. All these stones were mapped (Fig. 11a) and the percentage data of the areal extent of each lithology extracted with Rhinoceros software (Table 5).

Petrographic study of the thin-sectioned stones

White Carrara marble

This stone (samples 2E, 1S) corresponds to a pure calcite (sometimes partially dolomitic) fine-grained marble with isotropic fabric and Grain Boundary Shapes (GBS) mainly straight, in a homeoblastic and polygonal mosaic microstructure made of calcite crystals often forming triple points (120°). The Maximum Grain Size (MGS) is 0.36 mm. The few accessory minerals observed are pyrite, graphite and quartz (Fig. 3a–c), the latter also detected by XRPD analysis, as well as a limited amount of dolomite (Table 3). These petrographic features identify this material as *Carrara* marble, from the Italian Apuan Alps [23].

Grey crystalline Proconnesian marble

Another calcite marble is present (sample 9W), showing heteroblastic fabric, mortar microstructure and GBS mainly sutured and, secondarily embayed. It is a coarse-to medium-grain marble with MGS around 4.50 mm. The mineralogical composition comprises calcite with graphite as accessory mineral (Fig. 3d–f). XRPD analysis shows predominant calcite and rare quartz (Table 3). The samples are recognizable as Proconnesian marble fragments from the Island of Marmara [23].

Istrian stone

A compact sedimentary rock corresponding to Istrian Stone, a marine micritic limestone [24] to be classified as a carbonate mudstone [25, 26] were also identified (samples 3E, 5E, 5W, 8W). Very rare fragments of unidentifiable shells define the allochem constituents. Stylolites, as well as sedimentary joints, are frequent, with small deposits of clay minerals and iron oxides and hydroxides (hematite-limonite) often occurring along them (Fig. 3g–i). XRPD investigation confirmed the predominant calcite composition (only sample 5E shows scarce dolomite) coupled with traces of quartz (Table 3).

Ammonitico Rosso from Verona

This rock, recognised in samples 2N and 4N, is a nodular limestone with abundant bioclasts dispersed in an abundant micritic mud and rare spathic cement in which hematite is finely dispersed (Fig. 3j–l). The allochem constituents are ammonites (macroscopic), fragments of bivalves (pelagic lamellibranchs), planktonic foraminifera and echinoderms. The stone can be classified as biomicrite [24] or wackestone [25, 26]. XRPD analysis shows predominant calcite combined with scarce quartz (Table 3). All these characteristics are distinctive of *Ammonitico Rosso* from *Verona* [27, 28].

Venetian Scaglia Rossa

Finally, a marine micritic limestone with sparite limited as a filler of fossil footprints is also present (samples 1E, 1N, 3N, 1W). Allochem constituents are planktonic foraminifera, Globotruncana, Globigerinida. XRPD analysis detected only abundant calcite together with scarce presence of quartz (Table 3). The rock can be classified as biomicrite [24] or wackestone [17]) and belongs to the white variety of the Venetian *Scaglia Rossa* Formation, locally corresponding to the so-called “*Pietra di Prun*” or “*Pietra di Lessina*” or also “*lastame*” (Fig. 3m–o) [27, 28].

Macroscopically-defined stones

Porfido Rosso Antico (lapis porphyrites)

The rock of the two *rotae* (round plates) on either side of the central archway to the *Mercerie* was easily identified, by the naked eye, as the famous *Porfido Rosso Antico* or *lapis porphyrites* [30]; it is a volcanic rock (of the Paleozoic period) showing porphyritic texture, made of whitish to pink saussuritized plagioclase and rare blackish amphibole (ferro-hornblende) phenocrysts embedded in a purple glassy groundmass. The red–purple background colour is due to the presence of a combination of hematite and piemontite (the manganese-rich member of the epidote group) in the groundmass. *Porfido Rosso Antico* is typically classified as andesite-trachyandesite/dacite [30–32] and it originates from the *Mons Porphyrites*, a mountain massif today called Gebel Dokhan, located west of Hurghada in the Egyptian Eastern Desert.

Pavonazzetto Toscano marble

The slabs, located as the frame of the clock and the central archway, are attributable to *Pavonazzetto Toscano*. This is a fine-grained, calcite marble with dark purple magnetite-bearing layers; it dates to the Hettangian age and, like Carrara marble, originates from the Apuan Alps [15, 33].

Fior di Pesco (marmor chalcidicum)

The rock types of the *rotae* located at the top of the *bifore* of the third floor correspond macroscopically to *Fior di Pesco*, a deformed light-pink (the colour of “peach flower”) to purple-red cataclastic hematitic limestone. This colour of the rock is due to the dispersion of, sometimes manganeseiferous, hematite. The ancient quarries, nowadays largely destroyed by persistent cultivation, are located just north-west of the city of Eretria on the Island of Euboea (Greece).

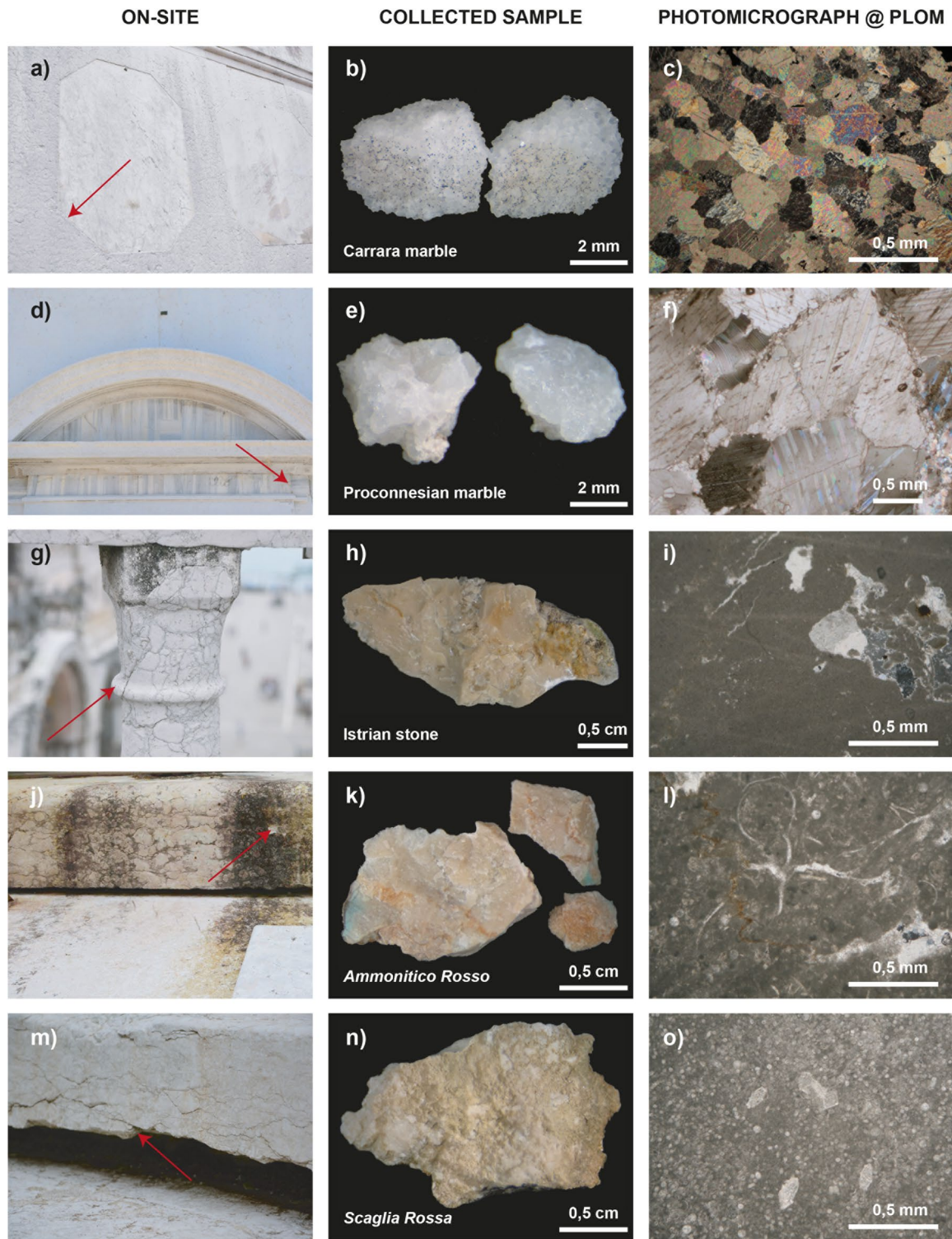


Fig. 3 Sampling points (red arrows), stereomicroscope photos, and transmitted polarized-light microscope microphotographs (crossed-polarised light) of: sample 2E, Carrara marble (a–c); sample 9W, Proconnesian marble (d–f); sample 5E, Istrian stone (g–i); sample 2N, Ammonitico Rosso from Verona (j–l); sample 1N, Scaglia Rossa (m–o)

Table 3 XRPD mineralogical composition (and semi-quantitative estimation) of the micro-samples of rocks and decay products

Minerals	Cal	MgCal	Dol	Gp	Qz	We	WM
Rocks							
1E	xxx				**		
1N	xxx				*		
1S	xxx	x			**		
1W	xxx				**		*
2N	xxx				*		
3E	xxx						
3N	xxx				**		
4N	xxx				**		
5E	xxx		**		**		
5S	xxx			x	**		
5W	xxx				**		
6E	xxx						
8W	xxx				**		
9W	xxx				*		
Black crusts							
2S	xxx			x			
4S_b				xxx	x	x	
5S-b				xxx	x	x	x
Patinas							
4W	xxx				**		
7E	xxx				*		
7W	xxx				*		
8E	xxx				**		

Mineral abbreviations after Whitney and Evans [29]: *Cal* calcite, *Dol* dolomite, *Gp* Gypsum, *Qz* quartz, *We* weddellite; WM = white mica. Other abbreviations: *MgCal* Mg-rich calcite. Relative quantity: xxx = very abundant; xx = abundant; x = present; ** = scarce; * = rare

Deterioration forms and their distribution

The most widely recognised deterioration forms divided into macro groups as indicated by ICOMOS [20], are as follows below.

Crack and deformation

In this group the most abundant morphologies are due to cracks, more specifically fractures (Fig. 4a, b), with deterioration level (DL) value between 1 and 2. The façade more afflicted by this phenomenon is on the southern side (Fig. 5a). Following, morphologies related to deformation, mainly as a bowing phenomenon (i.e., a convex deformation essentially due to thermal shocks) affect the median section of the marble slabs in particular and show DL 1 to 2 (Fig. 4c). The latter deterioration pattern is more evident on the eastern façade. A more intense deformation (DL 3) affects the extreme NE *lesene*, where one stone block appears to be slightly tilted (Fig. 4d).

Detachment

Only the southern façade, where salt crystallization and black crusts are more intense, features small areas of

blistering phenomena (Fig. 4e) with DL between 1 and 2. Moreover, both limestone and crystalline marbles panels exhibit disintegration features (i.e., intracrystalline decohesion and sugaring phenomena for marbles) (Fig. 4f); these morphologies are more common on the side façades (Fig. 5b) with DL of 1 or 2.

Features induced by material loss

The mapping revealed that the main forms belonging to this group are differential erosion with a DL of between 1 and 2, in particular as a consequence of a greater recession rate (due to a dissolution effect) of the fine-grained calcite portions of limestone (Fig. 6a, b) with respect to those with average-to-coarse grained carbonate. This decay morphology is more common in the eastern and western façades (Fig. 7a). Microkarst of slight intensity (DL 2) is also present, affecting all the small columns of the balustrades in Istrian Stone (Fig. 6c). Finally, missing parts with an intensity varying between very slight and very severe (DL 1 to 5) were identified; in particular, some *rotae* of *Fior di Pesco* are partially or completely missing.



Fig. 4 Crack and deformation: **a** fractures on a pillar base (southern façade), and **b** on the marble slabs decorating the doorframe arch (eastern façade); **c** faint convex deformation on marble slabs (western façade); **d** lestone deformation (southern façade). Detachment: **e** blistering phenomena (southern façade); **f** sugaring phenomena on marble slabs (western façade)

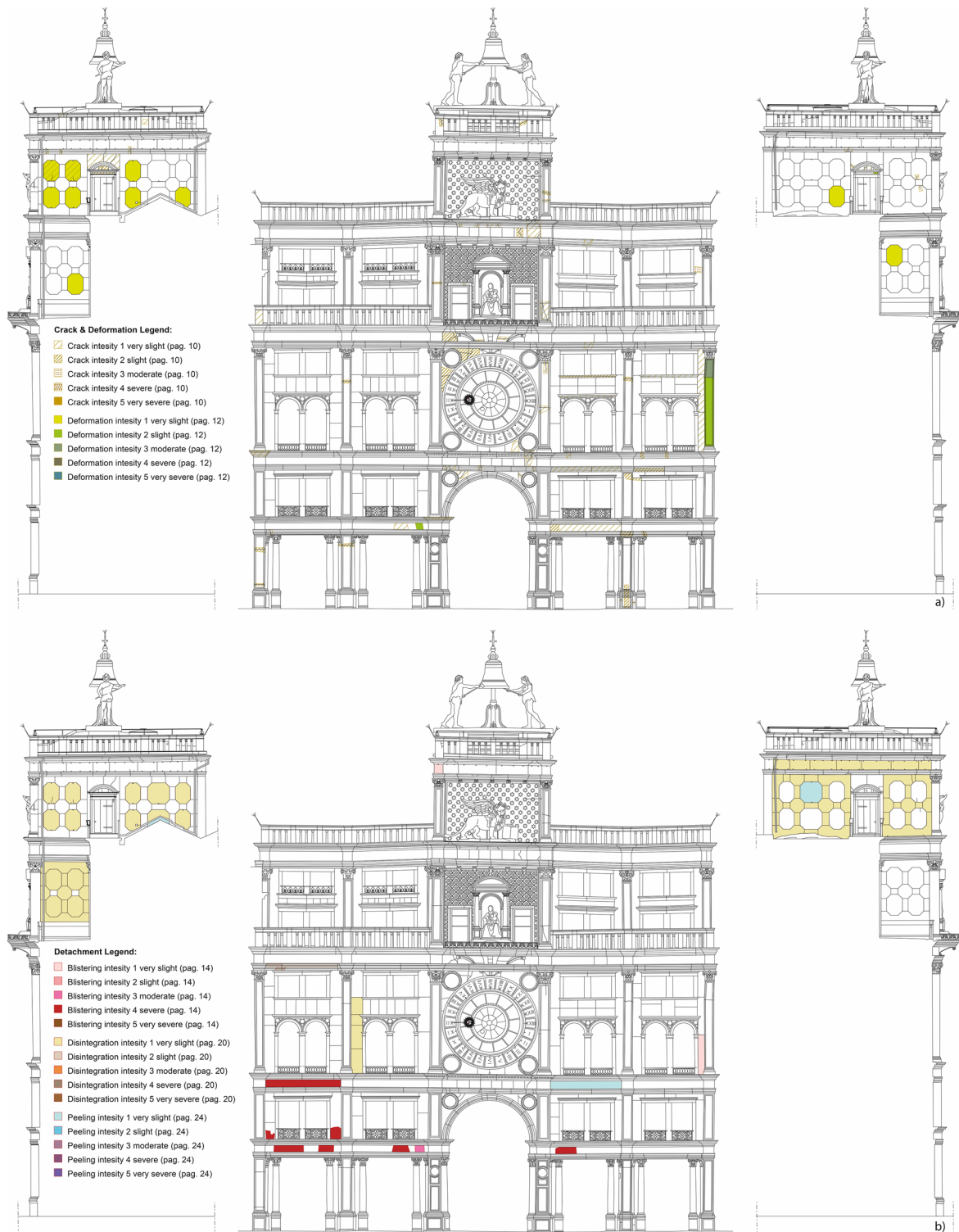




Fig. 6 Features induced by material loss: **a, b** differential erosion on *Ammonitico Rosso* from Verona slabs (eastern façade), **c** microkarst on Istrian Stone small columns (western façade). Discoloration and deposit: **d** black crusts on Istrian-stone Corinthian capitals (southern façade); **e** soiling on Scaglia Rossa slabs (western façade); **f** efflorescence on Istrian Stone small columns (western façade); **g** greenish staining on Istrian Stone (western façade); **h** yellowish patinas (southern façade)

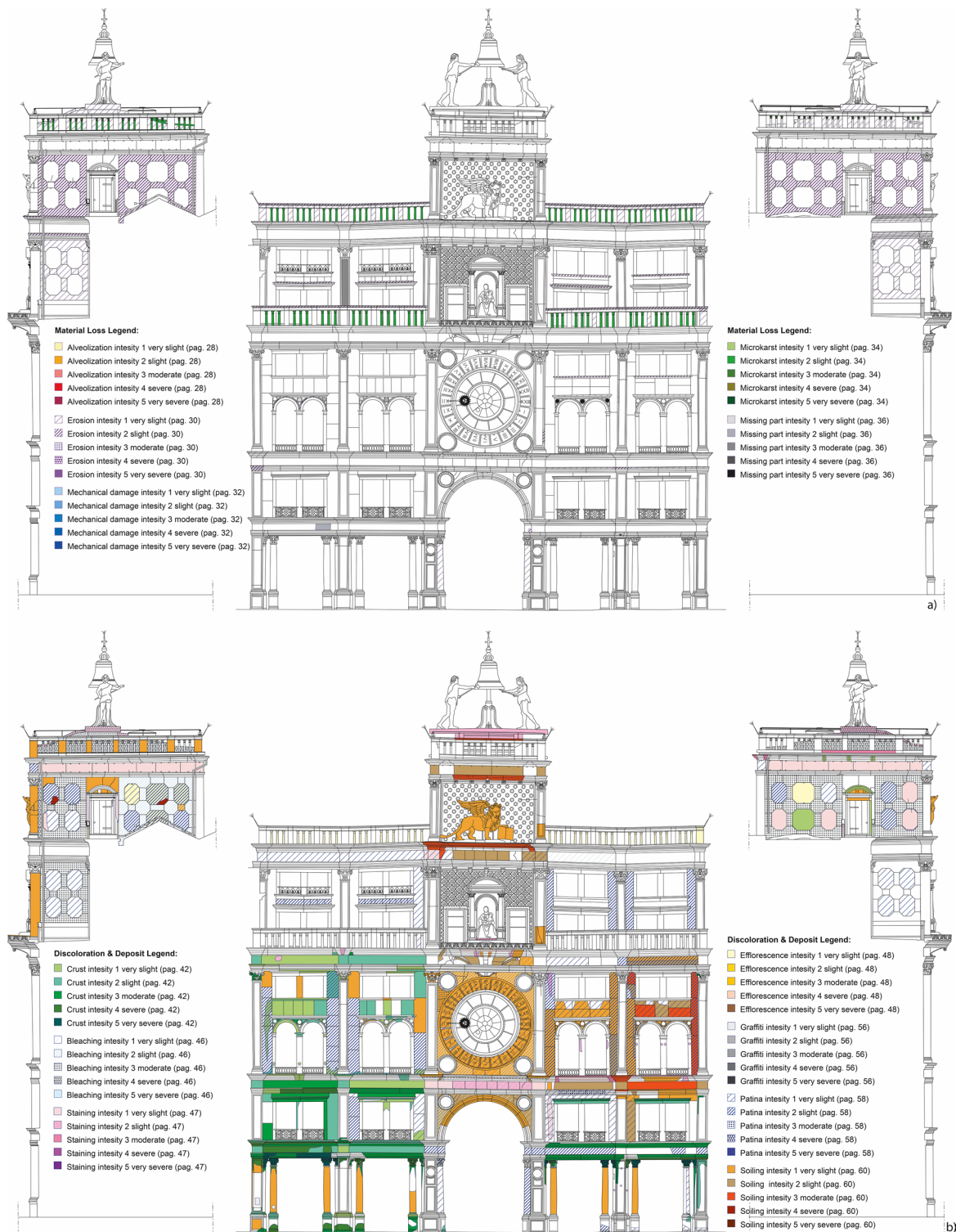


Fig. 7 Clock tower: maps of deterioration forms: **a** Features induced by material loss; **b** Discoloration and deposit

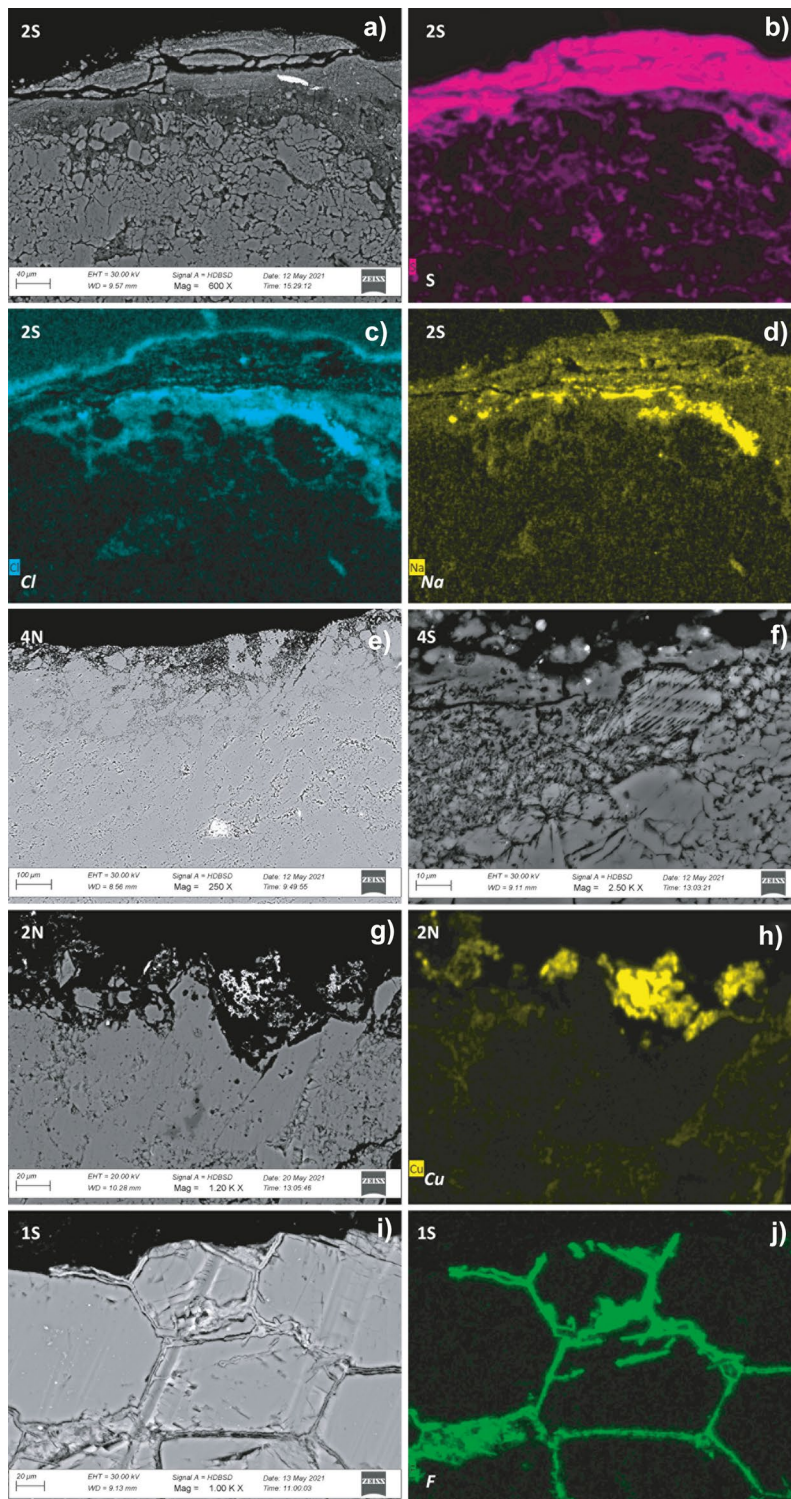


Fig. 8 **a** SEM-BSE image of the black crust in sample 2S, and elemental distribution maps of **b** sulphur (S, pink), **c** chlorine (Cl, light blue), and **d** sodium (Na, yellow); **e** SEM-BSE images of sample 4N where discoloration phenomenon are displayed; **f** SEM-BSE images of sample 4S showing micro-cracks in the surface crystals; **g** SEM-BSE image of staining deposits in sample 2N, and elemental distribution map of **h** Cu (copper, yellow); **i** SEM-BSE image of past treatment residue in sample 1S, and elemental distribution map of **j** F (fluorine, green)

Discoloration and deposit

For this group, there are quite frequent black crusts mainly in the western side of the ground floor of the southern façade (Fig. 7b), heavily afflicting the Corinthian capitals (Fig. 6d). XRPD, performed on samples 4S and 5S (Table 3), are consistent with the classic gypsum-based composition of the black crust incorporating atmospheric particulate (especially carbon particles, pollens and wind-blown quartz), also showing traces of weddellite oxalate [15, 34–37]. The intensity of this alteration morphology covers all the DL range from 1 to 5. Some samples also revealed the presence of sub-florescence testified by the presence of a layer between the stone and the black crust itself. SEM–EDS investigation showed high values of Cl and Na, indicating a recrystallization of halite (NaCl) (Fig. 8a–d).

Bleaching and staining (Fig. 7b) are the main discoloration features. In the former case, pink and red limestones (i.e., *Ammonitico Rosso* from *Verona* and *Scaglia Rossa*) have lost their hematitic pigments from the most superficial layers and change their colours to lighter hues, due to weathering, leaching and iron mobilisation [38]. This phenomenon is clearly revealed by BSE images of sample 4N where iron-bearing minerals are absent from the surface and appear in greater concentration at a depth of around 400–500 µm (Fig. 8e). This pattern is more present in the two side façades, ranging in DL from 1 to 4.

On the other hand, staining creates greenish and reddish localized halos due respectively to the dispersion of copper from the statues of the Moors (Fig. 6g), and iron products (mainly hydroxides), deriving from the weathering and dispersion of metallic elements of inserts. The elemental mapping by SEM–EDS of samples with macroscopically green surface deposits revealed the presence of Cu, Cl and Na (Fig. 8g, h). The DL values of this

decay product range from 1 to 3. Another type of deposit is represented by efflorescence which appears mainly as whisker-like crystals (Fig. 6f) of very slight and slight intensity (corresponding to DL 1 and 2, respectively) on the surface of the small columns of the balustrades (Fig. 7b). Table 4 lists the anions detected by IC that identify the main salts constituting the different types of efflorescence. The samples were tested for all the following ions: fluorides, chlorides, nitrites, bromides, nitrates, phosphates, sulphates, lithium, sodium, ammonium ion, potassium, magnesium, calcium. The main contents are of chlorides and sulphates for the anions, and sodium and calcium for the cations, compositions that are consistent with halite (NaCl) and gypsum (CaSO₄·2H₂O) crystallizations. In addition, sample 5E showed a significant amount of magnesium, which could be linked to the presence of dolomite (Ca,Mg(CO₃)₂), a Mg and Ca carbonate, in this sample, as also indicated by its XRPD (Table 3). Finally, all the samples show significant calcium content, which can easily be linked to the carbonate nature of most of the samples and/or their stone substrates.

Patinas, resulting from the ageing of ancient treatments, appear as a yellowish colour alteration of crystalline marble slabs and columns/pilasters (Fig. 6h). The DL values of this decay product range from 1 to 3. The study performed by FTIR compared with EDS elemental mapping enabled the nature of the past treatments applied on the marble columns to be determined with great accuracy. The abundance of fluorine diffused in the superficial micro-cracks and detected by EDS (Fig. 8i, l), combined with the recognition by FTIR of an acrylic-siloxane mixture (3432 cm⁻¹ due to ν Si–OH, 2959–2928–2873 cm⁻¹ related to ν C–H chemical bond, 1737 cm⁻¹ linked to ν C=O, 1260 cm⁻¹ related to ν Si–(CH₃), 1161 cm⁻¹ linked to ρ C–H and

Table 4 Anions and cations obtained by IC and expressed as percentages by weight

Sample	1E	1N	1W	2N	2S	4N	5E	5S	5W	7E	8W
Anions											
Fluoride	–	–	0.01	–	0,01	–	–	0,01	–	–	–
Chloride	0.02	0.03	0.03	0.03	0,13	0.03	0.03	0,07	0,05	0,04	0.03
Nitrate	–	–	–	–	0,05	–	–	0,04	0,06	0,03	–
Sulphate	0.03	0.03	–	0.03	<i>1,09</i>	0.03	–	<i>0,68</i>	<i>0,13</i>	0,05	0.04
Cations											
Sodium	0.04	0.03	0.02	0.04	0.26	0.03	0.04	0.11	0.02	0.04	0.04
Ammonium	0.08	0.10	0.05	0.09	–	0.06	0.07	0.11	0.10	0.09	0.09
Potassium	0.08	–	0.08	–	–	0.10	0.09	0.14	–	–	–
Magnesium	0.13	0.05	0.38	0.07	0.02	0.15	<u>0.59</u>	0.08	0.28	0.13	0.66
Calcium	1.63	1.66	1.44	1.66	<i>5,06</i>	1.82	1.58	3.03	2.36	1.75	2.19

In **bold**, ions connected with the presence of Halite (NaCl); in *italics*, ions connected with the presence of Gypsum (CaSO₄·2H₂O); underlined, ions connected with the presence of Mg-bearing carbonates

1115–1033–1007 cm^{-1} attributed to ν_s Si–O–Si), suggests the use of fluosilicates and acrylic-siloxane products on the stone surfaces during two different restoration interventions (samples 1S, 6W). Indeed, from the EDS map, the silicon distribution in the samples is limited to the surface and in few spots of the superficial micro-cracks, suggesting the application of fluosilicate previous to that of acrylic-silicone resin. The presence of peaks related to acrylic-siloxane compounds was also detected in sample 6E from the eastern façade. The characteristic peaks of calcium oxalate dihydrate

(weddellite) have been also detected (3400 cm^{-1} due to ν O–H, 1646 cm^{-1} linked to ν C=O, 1327 cm^{-1} attributed to ν C–O and 798 cm^{-1} corresponding to δ C–H) in samples 1S, 3S, 6E and 4W. This material probably results from the mineralization process of historical organic consolidation treatments [39] rather than from biological attack [40, 41].

Finally, soiling is the most widespread deterioration morphology in the whole building (Fig. 6e). It appears as a tenuous blackish-grey layer (DL between 1 and 4) that confers a dirty appearance to the stone.

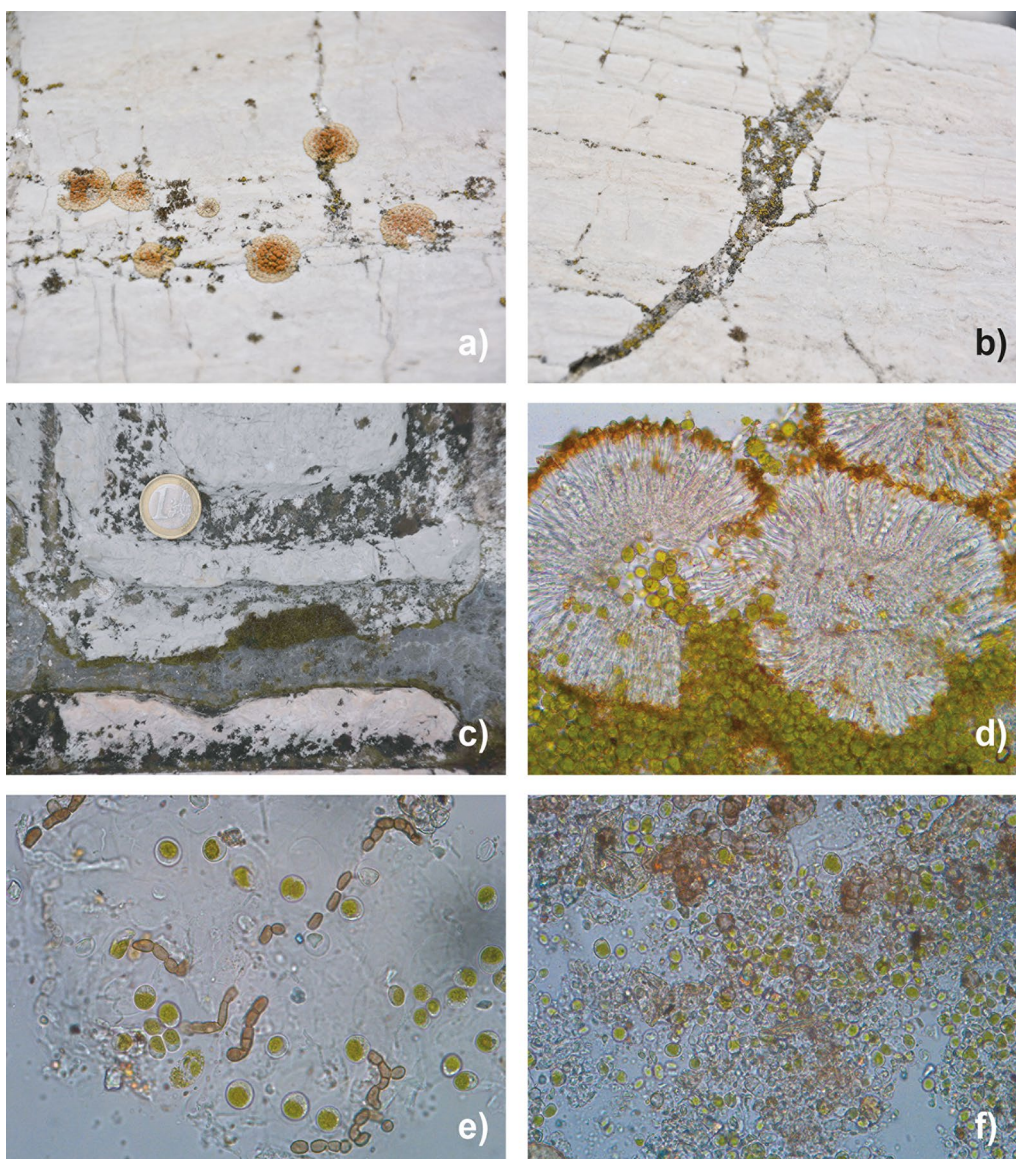


Fig. 9 **a, b** Lichen and fungus colonization (western façade); **c** moss colonization (eastern façade); **d** optic microscopy microphotographs of fresh slides of sample 9E showing lichen apothecia in cross-section; **e** optic microscopy microphotographs of fresh slides of sample 3W showing hyphae of meristematic fungi and cells of green algae; **f** optic microscopy microphotographs of fresh slides of sample 1W green algae cells, cyanobacteria colonies and a few fungal hyphae.

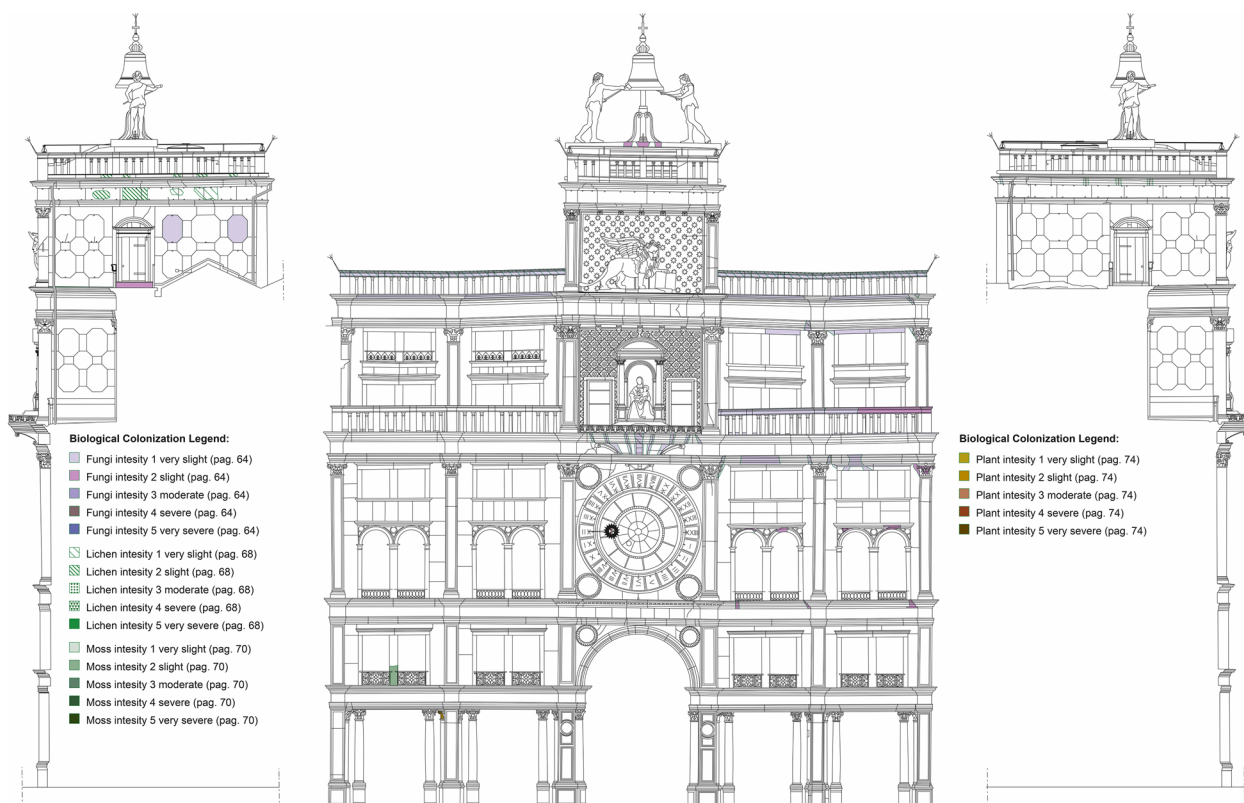


Fig. 10 Clock tower: map of deterioration forms of biological colonization

SEM-BSE images obtained from extensive SEM investigations revealed peculiar micro-damage patterns in the Carrara marble samples from the ground floor columns. These are micro-cracks concentrated only in the superficial crystals clearly guided by the cleavage planes of the mineral (Fig. 8f).

Biological colonization

The colonization of lichens and fungi (DL between 1 and 2) is mainly found on Istrian Stone (Fig. 9a, b) with homogeneous distribution on the three façades (Fig. 10). Rarely, mosses were identified and when present are visually impactful (Fig. 9c); they were found mainly in the walkways between the balustrades of the two wings of the building so they cannot be mapped on the elevations. More in detail, five different microorganisms were detected by OM investigation, as follows below.

Caloplaca saxicola (Hoffm.) Nordin [42] Crusty lichen with lecanorine apothecia having a bright orange disc and slightly lighter margins (Fig. 9d). The thallus is placodomorphic and pale yellow in colour. Chemical test with potassium hydroxide (KOH) solution gives a positive result (K+) [21].

Candelariella aurella (Hoffm.) Zahlbr [42] Crusty lichen with yellow apothecia and blurred thallus. Some apothecia are covered with a blackish patina while others have brownish branching. Chemical test with potassium hydroxide solution (KOH) gives negative result (K-).

Meristematic fungi Blackish patina (Fig. 9c) and brownish branching due to meristematic fungi, whose hyphae are arranged in chain. Brown colour indicates the presence of melanin [43]. This biological material often appears in combination with lichens and algae (Fig. 9e).

Moss This refers to plants belonging to the bryophyte division and more specifically to the class of mosses. Under the stereomicroscope it is possible to observe the gametophyte, i.e., the green part of the moss consisting of leaflets, and the sporophyte of which we can see the capsules, or urns, containing the spores, which are carried on top by filaments known as setae [43].

Green algae Investigation of greenish patinas identified green algae cells combined with cyanobacteria colonies and a few fungal hyphae (Fig. 9f) [43].

From the maps obtained, percentage data of the areal extent of each morphology were also extracted using

Table 5 Areal percentage coverage of each weathering form and of five TDR levels

Group of weathering forms	Group of weathering forms					% Area				
	DL	South Façade	East Façade	West Façade	Total	DL	South Façade	East Façade	West Façade	Total
Crack and Deformation	1	n.a	n.a	n.a	n.a	1	0,2	0	0	0,1
	2	n.a	n.a	n.a	n.a	2	0	0	0	0
	3	n.a	n.a	n.a	n.a	3	0	0	0	0
	4	n.a	n.a	n.a	n.a	4	0,8	0	0	0,6
	5	n.a	n.a	n.a	n.a	5	0	0	0	0
Deformation	1	2,8	8,1	2,0	3,4	1	0,5	25,4	13,1	5,4
	2	0,4	0	0,1	0,3	2	0,1	0	0	0,1
	3	0,1	0	0	0,1	3	0	0	0	0
	4	0	0	0	0	4	0	0	0	0
	5	0	0	0	0	5	0	0	0	0
Discoloration and deposit	1	2,1	0	2,5	1,9	1	0,3	0,2	1,5	0,5
	2	3,1	0	0	2,3	2	0	0	0	0
	3	2,8	0	0	2,1	3	0	0	0	0
	4	0,9	0	0	0,6	4	0	0	0	0
	5	0,4	0	0	0,3	5	0	0	0	0
Bleaching	1	1,0	0	0	0,7	1	2,3	11,3	13,1	4,9
	2	0,9	7,9	0	1,7	2	1,4	14,7	16,0	5,1
	3	0,1	11,3	15,7	3,6	3	0	0	0	0
	4	0	5,9	4,2	1,3	4	0	0	0	0
	5	0	0	0	0	5	0	0	0	0
Staining	1	0,6	6,1	8,7	2,4	1	0	0	0	0
	2	1,1	1,1	1,1	1,1	2	2,3	1,1	1,2	2,0
	3	0,1	0	0,8	0,2	3	0	0,3	0,3	0,1
	4	0	0	0	0	4	0	0	0	0
	5	0	0	0	0	5	0	0	0	0
Efflorescence	1	0,6	4,6	5,8	1,8	1	0,1	0	0	0,1
	2	0	0	0	0	2	0,1	0	0	0,1
	3	0	0	0	0	3	0	0,1	0	0
	4	0	0	0	0	4	0	0	0	0
	5	0	0	0	0	5	0	0	0	0

Table 5 (continued)

Group of weathering forms	Group of weathering forms					DL	Group of weathering forms	% Area				
	DL	South Façade	East Façade	West Façade	Total			DL	South Façade	East Façade	West Façade	Total
Graffiti	1	0	0	0	0	0	Biological coloniza- tion	0.6	0	0	0.7	
	2	0	0	0	0	0		1.1	0	0	0.2	
	3	0	0	0	0	0		0	0	0	0	
	4	0	0	0	0	0		0	0	0	0	
	5	0	0	0	0	0		0	0	0	0	
Patina	1	6.1	7.1	14.2	7.3	7.3	Fungus	2.0	0	0	2.0	
	2	10.9	5.9	5.0	9.5	9.5		0.9	0	0	0.4	
	3	0	0	0	0	0		0	0	0	0	
	4	0	0	0	0	0		0	0	0	0	
	5	0	0	0	0	0		0	0	0	0	
Soiling	1	8.4	7.9	0.6	7.3	7.3	Moss	0	0	0.2	0	
	2	2.7	0	0	2.0	2.0		0	0	0	0	
	3	1.7	0	0	1.2	1.2		0	0	0	0	
	4	0	0.3	0	0	0		0	0	0	0	
	5	0	0	0	0	0		0	0	0	0	
Stones	Ammonitico Rosso fV	0.8	5.3	4.3	1.8	1.8	Plant	0	0	0	0	
	Scaglia Rossa	0.1	20.3	22.3	5.7	5.7		0	0	0	0	
	Istrian Stone	48.6	43.1	39.9	46.7	46.7		0	0	0	0	
	Proconnesian Marble	19.7	6.2	7.2	16.3	16.3		0	0	0	0	
	White Carrara Marble	3.1	14.7	15.1	6.2	6.2		0	0	0	0	
Pavonazzetto Toscano Marble	2.1	0	0	1.5	1.5	TDR	19.9	29.9	27.1	27.1		
Fior di Pesco	0.1	0	0	0.1	0.1		18.9	6.0	16.6	16.6		
Porfido Rosso Antico	0.1	0	0	0.1	0.1		11.7	16.9	7.9	7.9		
Mortar-based materials	1.5	0	0	1.1	1.1		6.2	4.2	2.6	2.6		
								0	0	0.3	0.3	

"n.a." stands for "not applicable"

Rhinoceros software. The same measurement was also performed on the TDR map. Data are reported in Table 5.

Discussion

Distribution of stones

Observations on the use of stone types in relation to the types of architectural elements reveal an attentive use of different lithotypes in building the Clock Tower. In general, considerable use was made of stone from local sources or stone that was widely used in Venice (Istrian Stone, *Ammonitico Rosso* from Verona, *Scaglia Rossa*). In particular, the most valuable are located on the original tower, built independently in 1499, whereas the most common are more abundant on the two subsequent wings of the building, added in 1506, then elevated in the mid-eighteenth century, in order to create a city planning and scenographic unicum of St. Mark's Square. In particular, most of the columns and buttresses are made of Istrian Stone, except for those on the ground floor, where the more precious *white Carrara marble* is used. *Proconnesian marble* is widely used in slabs, framed by the Istrian Stone buttresses, covering and enriching the two wings. The decorative elements that stand out are the Egyptian *Lapis porphyrites* in the two *rose* windows in the centre of the southern façade, and, of course, the precious pattern created by the *Pavonazzetto Toscano* marble around the clock on the same façade. The only stone decoration on the two wings is the series of *rotae* made of *Fior di Pesco* adorning the mullioned windows of the second floor. The pink-whitish variety of *Ammonitico Rosso* from Verona seems to be limited to the base of the two Moors, while the other local stone, *Scaglia Rossa*, frames the Carrara marble panels on the eastern and western façades and probably forms the base for the *Madonna* statue. The lithological map is available in Fig. 11a.

Distribution of the deterioration morphologies on the monument

The in-depth study of the mapping carried out for the different types of deterioration morphology as well as that for the TDR (Total Deterioration Rank, Fig. 11b) enabled us to develop some particular observations on the distribution of decay on the monument surfaces.

The most noticeable aspect is certainly that, with reference to the southern façade, the materials of the central area (the Tower itself) are characterised by a much lower level of deterioration than those of the two wings and the two side façades. The TDR here reaches a maximum value of 3 and that only in a small area of the clock decoration, due to a system of cracks affecting the *Pavonazzetto Toscano* marble. Indeed, the general tendency here, as regards intensity, is not to exceed 1 and 2. On the contrary, the two side wings show marked signs of

deterioration with peaks of TDR equal to 5 in the capitals of the columns on the ground floor. This is linked to the spread of significant black crusts in these same areas. It is also true that the microclimate in the colonnade of the Tower is certainly more favourable to the development of extensive deposits of black crusts, given the more difficult ventilation and the protected position of the Corinthian capitals (in which the phenomenon is at its highest levels) from the action of rain and wind. The general tenor of the wings, however, is between 2 and 3. The stone materials of the side façades are characterised by TDR values of between 3 and 4 due to the widespread and pervasive development of patinas and bleaching phenomena.

The different degree of the stone-conservation between the Tower and the wings is also attributable to the fact that the various portions have undergone different restoration and cleaning actions over the years. In particular, one of the most recent restorations in 2000 only involved the Tower, completely excluding the side wings. This is because the two wings, also divided into portions, belong to different private entities, whereas the Tower is owned and supervised by the Municipality of Venice. It is therefore difficult to carry out a single, homogeneous intervention, mainly for economic reasons. Consequently, the uneven management of the entire building has partially distorted this unitary essence, enhancing and conserving the central part with greater care and neglecting the two lateral portions.

Evidence of past restoration actions

Several pieces of evidence allow at least two previous consolidation treatments to be identified, the first applied on the columns of the portico on the ground floor and on the balustrades of the western terraces, the second on the eastern façade. The use of fluosilicates is ascertained by SEM, though no archive documents confirmed their application. Some historical documents indicate an experimental phase in the use of these inorganic consolidants in Venice during the 1880s [44] and their application during restoration treatments in 1892 for the consolidation of *Pilastrini acritani* [45] and in 1968 using the Sanpaolesi method for the consolidation of Ca' d'Oro [46]. The lack of documents precludes definition of the date of the application on the Tower.

The application of acrylic-silicone compounds was probably carried out at a later stage. Indeed, the use of this mixture in Venice is attested in the second half of the XX century. Their use may therefore be attributed to more recent interventions. Also in this case, the lack of information accessible to the authors prevents them from accurately dating the intervention.

Finally, evidence of cleaning treatments could be related to the micro-fractures recognised through

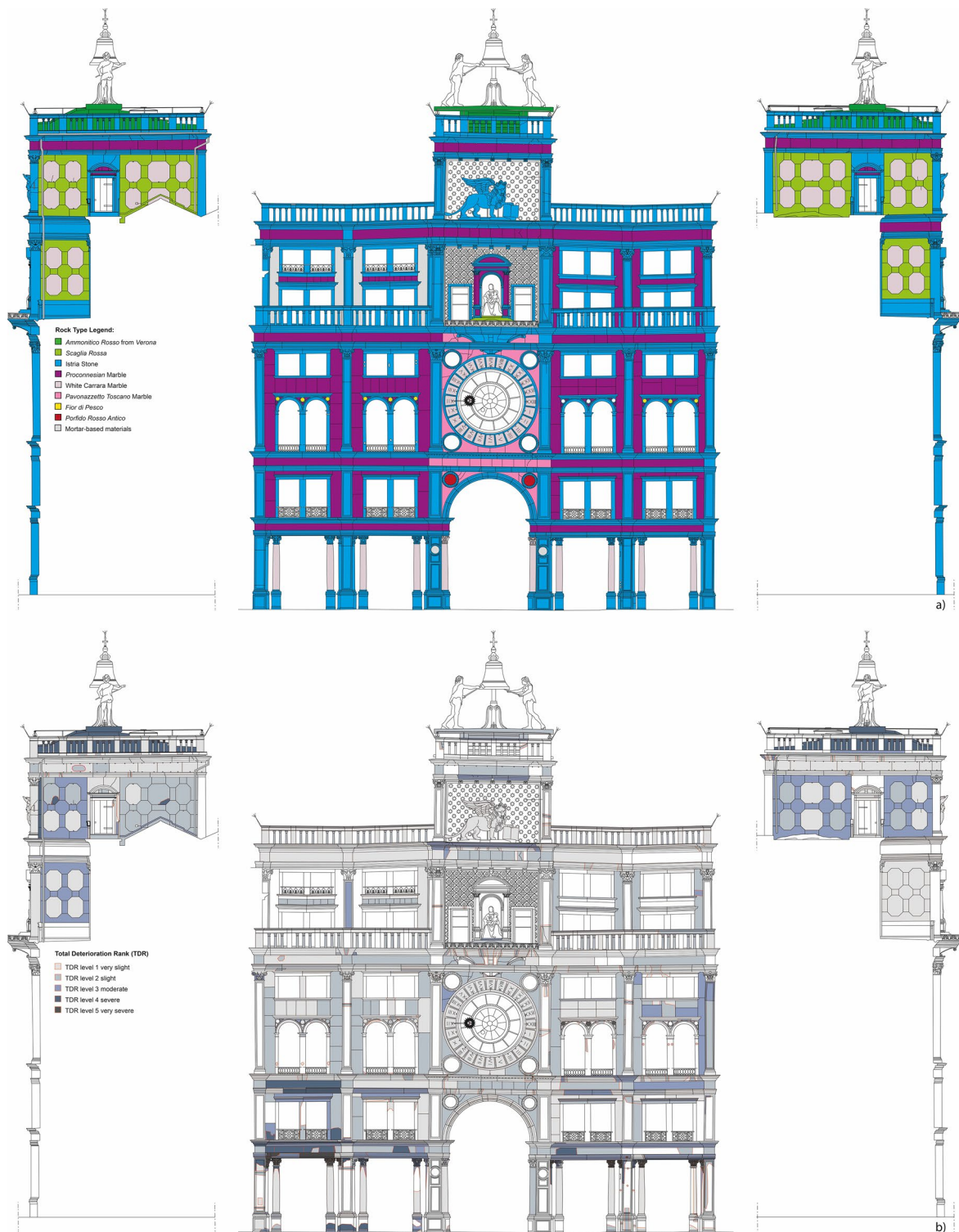


Fig. 11 Clock tower maps of: **a** Rock types and lithoid materials; **b** Total Deterioration Rank (TDR)

SEM-BSE image on the surface crystals of calcite in the white marble of the columns of the mid-eighteenth century colonnade. Studies on conservation procedures [47]

suggest that this damage could be an unintentional secondary effect of the laser cleaning procedure performed on the stone surface to remove deposits. This technique

seems to induce the calcite crystals to break following the natural cleavage directions.

Conclusions

The study and mapping of the Clock Tower allowed for a series of general observations to be made on the stylistic choices of the building stones and the state of preservation of the monument. As regards deterioration, useful considerations were guided by the simple and intuitive approach using the Total Deterioration Rank (TDR) proposed here. This indicator, coupled with the proposed approach that involves the application of carefully predetermined parameters for the macroscopic assessment of the intensity of each degradation form, proved to be a practical and relatively quick tool for the assessment of the conservation status of the whole building. From the point of view of the materials used, their recognition and mapping made it possible to highlight that the building made extensive use of stone obtained from local sources or widely used in Venice (e.g., Istrian Stone, *Ammunitico Rosso* from Verona, *Scaglia Rossa*), as well as precious materials (e.g., *Pavonazzetto Toscano*, *Lapis porphyrites*) thriftily and effectively used to enrich the central part of the Tower, enclosing them in a refined homogenous frame of *Proconnesian marble*.

As regards the state of conservation, the analysis of the maps in particular allowed us to recognize a marked lack of homogeneity in the preservation of the building as a whole, thus highlighting the need for a more unified approach to the preservation of the asset as an important heritage item in the Venetian landscape. This is due to the uneven management, especially in recent decades, of the entire building, which belongs to different institutions. Indeed, the state of deterioration found in the stone materials of the two lateral bays, and particularly in the mid-eighteenth century colonnade on the ground floor, is certainly more marked and in need of attention. It is also true that the microclimate in the colonnade of the Tower is certainly more favourable to the development of extensive deposits of black crusts, given the more difficult ventilation and the protected position of the Corinthian capitals (in which the phenomenon is at its highest levels) from the action of rain and wind.

In addition to this, the detailed analysis has enabled some observations to be made on past treatments. Of particular interest is undoubtedly the presence of fluosilicates, which belong to an important parenthesis in the history of restoration and conservation and will be the subject of further investigation in the Venetian area, especially in St. Mark's Square.

Acknowledgements

The authors are grateful to the *Soprintendenza Archeologia, belle arti e paesaggio per il Comune di Venezia e Laguna* for allowing the sampling of materials; the City of Venice (Italy) and the *Fondazione Musei Civici di Venezia*

for guaranteeing and facilitating access to the monument during survey and sampling operations. A special acknowledgement is also due to Dr. Foriana Majerle for the study of biological patinas and Dr. Luana Scarpel for the Rhinoceros software elaboration.

Author contributions

Conceptualization, RP, and FA; Methodology, RP, and ET; Validation, RP, and FA; Formal Analysis, RP, and ET; Investigation, RP, ET, LM, and GZ; Writing—Original Draft Preparation, RP; Writing—Review & Editing, RP, FA, LM, and ET; Visualization, RP; Supervision, FA; Project Administration, FA, and CM; Funding Acquisition, FA.

Funding

This work was carried out and made accessible as open access thanks to the funding provided by the HYPERION project supported by the European Union's Framework Programme for Research and Innovation (Horizon 2020) under Grant Agreement number 821054.

Data availability

The data presented in this study are available on request from the corresponding author.

Declarations

Competing interests

The authors declare that they have no conflict of interest.

Received: 16 December 2022 Accepted: 19 March 2023

Published online: 16 May 2023

References

- Sanudo M, Labalme PH, Sanguineti White L. Venice, città excelentissima: selections from the Renaissance diaries of Marin Sanudo. Baltimore: Johns Hopkins University Press; 2008.
- Delgado Rodrigues J. Defining, mapping and assessing deterioration patterns in stone conservation projects. *J Cult Herit*. 2015;16:267–75. <https://doi.org/10.1016/j.culher.2014.06.007>.
- Antonelli F, Savalli A, Cantisani E, Fratini F, Giamello M, Lezzerini M, Pechioni E, Tesser E. Multianalytical approach to diagnosis and conservation of building materials: the case of Punta Troia Castle in Marettimo (Aegadian Islands—Sicily, Italy). *Appl Phys A Mater Sci Process*. 2016. <https://doi.org/10.1007/s00339-016-9803-6>.
- Freire-Lista DM, Fort R. Historical city centres and traditional building stones as heritage: Barrio de las Letras, Madrid (Spain). *Geoheritage*. 2019;11:71–85. <https://doi.org/10.1007/s12371-018-0314-z>.
- Piovesan R, Maritan L, Meneghin G, Previato C, Baklouti S, Sassi R, Mazzoli C. Stones of the façade of the Sarno Baths, Pompeii: A mindful construction choice. *J Cult Herit*. 2019;40:255–64. <https://doi.org/10.1016/j.culher.2019.04.010>.
- Theodoridou M, Török Á. In situ investigation of stone heritage sites for conservation purposes: a case study of the Székesfehérvár Ruin Garden in Hungary. *Prog Earth Planet Sci*. 2019. <https://doi.org/10.1186/s40645-019-0268-z>.
- Izzo F, Furno A, Cilenti F, Germinario C, Gorrazi M, Mercurio M, Langella A, Grifa C. The domus domini imperatoris Apicii built by Frederick II along the Ancient Via Appia (southern Italy): an example of damage diagnosis for a Medieval monument in rural environment. *Constr Build Mater*. 2020. <https://doi.org/10.1016/j.conbuildmat.2020.119718>.
- Thornbush MJ, Viles HA. Photo-based decay mapping of replaced stone blocks on the boundary wall of Worcester College. Oxford. *Geol Soc Spec Publ*. 2007;271:69–75. <https://doi.org/10.1144/GSL.SP.2007.271.01.08>.
- Grifa C, Barba S, Fiorillo F, Germinario C, Izzo F, Mercurio M, Musmeci D, Potrandolfo A, Santoriello A, Toro P, Langella A. The Domus of Octavius Quartio in Pompeii: damage diagnosis of the masonries and frescoed surfaces. *International Journal of Conservation Science*. 2016;7:885–900.
- Lezzerini M, Antonelli F, Columbu S, Gadducci R, Marradi A, Miriello D, Parodi L, Secchiari L, Lazzeri A. Cultural heritage documentation and

- conservation: three-dimensional (3D) laser scanning and geographical information system (GIS) techniques for thematic mapping of facade stonework of St. Nicholas Church (Pisa, Italy). *Int J Archit Herit*. 2016;10:9–19. <https://doi.org/10.1080/15583058.2014.924605>.
11. Karachaliou E, Georgiou E, Psaltis D, Stylianidis E. UAV for mapping historic buildings: from 3D modelling to BIM. *ISPRS Ann Photogram Remote Sens Spat Inf Sci*. 2019;42:397–402. <https://doi.org/10.5194/isprs-archi-ves-XLII-2-W9-397-2019>.
 12. Puy-Alquiza MJ, OrdazZubia VY, Aviles RM, Salazar-Hernández MDC. Damage detection historical building using mapping method in music school of the University of Guanajuato, Mexico. *Mech Adv Mater Struct*. 2021;28:1049–60. <https://doi.org/10.1080/15376494.2019.1629049>.
 13. Fitzner B, Heinrichs K. Damage diagnosis at stone monuments—Weathering forms, damage categories and damage indices. *Acta Univ Carol Geol*. 2001;45:12–3.
 14. Fitzner B, Heinrichs K, la Bouchardiere D. Limestone weathering of historical monuments in Cairo. Egypt. *Geol Soc Spec Publ*. 2002;205:217–39. <https://doi.org/10.1144/GSL.SP.2002.205.01.17>.
 15. Antonelli F, Lazzarini L, Cancelliere S, Tesser E. Study of the deterioration products, gilding, and polychromy of the stones of the Scuola Grande di San Marco's façade in Venice. *Stud Conserv*. 2016;61:74–85. <https://doi.org/10.1179/2047058415Y.0000000004>.
 16. Tesser E, Lazzarini L, Ganzerla R, Antonelli F. The decay of the polysiloxane resin Sogesil XR893 applied in the past century for consolidating monumental marble surfaces. *J Cult Herit*. 2017;27:107–15. <https://doi.org/10.1016/j.culher.2017.03.001>.
 17. Tesser E, Antonelli F. Evaluation of silicone based products used in the past as today for the consolidation of Venetian monumental stone surfaces. *Mediterr Archaeol Archaeom*. 2018;18:159–70. <https://doi.org/10.5281/zenodo.1285902>.
 18. Sgobbi M, Brimblecombe P, Grossi C, Biscontin G, Zendri E. Surface stratigraphy on limestone of Venetian palaces. *J Archit Conserv*. 2010;16:51–70. <https://doi.org/10.1080/13556207.2010.10785075>.
 19. Tesser E, Lazzarini L, Bracci S. Investigation on the chemical structure and ageing transformations of the cycloaliphatic epoxy resin EP2101 used as stone consolidant. *J Cult Herit*. 2018;31:72–82. <https://doi.org/10.1016/j.culher.2017.11.002>.
 20. ICOMOS, ISCS, ICOMOS-ISCS: Illustrated glossary on stone deterioration patterns, XV, ICOMOS, Paris, France, 2008.
 21. Nimis P, Monte M, Mauro T. Flora e Vegetazione Lichenica di Aree Archeologiche del Lazio. *Stud Geobot*. 1987;7:3–161.
 22. Nimis PL. I macrolicheni d'Italia. Chiavi analitiche per la determinazione. Gortania. 1986;8:101–220.
 23. Antonelli F, Lazzarini L. An updated petrographic and isotopic reference database for white marbles used in antiquity. *Rendiconti Lincei*. 2015;26:399–413. <https://doi.org/10.1007/s12210-015-0423-4>.
 24. Folk RL. Spectral subdivision on limestone types. In: *Classification of Carbonate Rocks-A Symposium*, 1962: pp. 62–84.
 25. Dunham RL. Classification of carbonate rocks according to depositional texture: in Northern Iraq, Arabian Gulf, Geology and Productivity. AAPG, Foreign Reprint Series; 1962.
 26. Embry AF, Klovan JE. A late Devonian reef tract on northeastern Banks Island, NWT. *Bull Can Pet Geol*. 1971;19:730–81.
 27. Bosellini A, Carraro F, Corsi M, De Vecchi GP, Gatto GO, Maroda R, Turani C, Ungaro S, Zanetti B. Note illustrative della Carta Geologica d'Italia alla scala 1:100 000: Foglio 49 "Verona," Servizio Geologico d'Italia. 1967; pp. 1–61.
 28. Albertini G. Geologia dei marmi veronesi. In: Rossini F (Ed.), *I Marmi a Verona*, Associazione Marmisti Veronesi AS.MA.VE, 1991: pp. 28–42.
 29. Whitney DL, Evans BW. Abbreviations for names of rock-forming minerals. *Am Miner*. 2010;95:185–7. <https://doi.org/10.2138/am.2010.3371>.
 30. Gnoli R, Ortolano G, Pensabene P, Claussen PC, Tuena F, Napoleone C, Marchei MC, Pettinau B, Bozzini P, Sironi A. *Marmi antichi*, De Luca, 1992: pp. 342. ISBN 9788880161813
 31. Lazzarini L. Pietre e marmi antichi. Natura, caratterizzazione, origine, storia d'uso, diffusione, collezionismo, CEDAM, 2004: pp. 194. ISBN 9788813250218
 32. Price MT. *Atlante delle pietre decorative*. Guida tecnica illustrata, Ediz. Illu, Hoepli, 2008: pp. 288. ISBN 9788820339623
 33. Lazzarini L. Il pavonazetto toscano a venezia e il suo deterioramento con un esempio marciano. In: Vio E, Lepschy A (Eds.), *Scienza e Tecnica Del Restauro Della Basilica Di San Marco*, Istituto Veneto di Scienza, Lettere ad Arti, Venice, 1999: pp. 651–665.
 34. Maravelaki-Kalaitzaki P. Black crusts and patinas on Pentelic marble from the Parthenon and Erechtheum (Acropolis, Athens): Characterization and origin. *Anal Chim Acta*. 2005;532:187–98. <https://doi.org/10.1016/j.jaca.2004.10.065>.
 35. La Russa MF, Fermo P, Comite V, Belfiore CM, Barca D, Cerioni A, De Santis M, Barbagallo LF, Ricca M, Ruffolo SA. The Oceanus statue of the Fontana di Trevi (Rome): the analysis of black crust as a tool to investigate the urban air pollution and its impact on the stone degradation. *Sci Total Environ*. 2017;593–594:297–309. <https://doi.org/10.1016/j.scitotenv.2017.03.185>.
 36. Comite V, Pozzo-Antonio JS, Cardell C, Randazzo L, La Russa MF, Fermo P. A multi-analytical approach for the characterization of black crusts on the facade of an historical cathedral. *Microchem J*. 2020. <https://doi.org/10.1016/j.microc.2020.105121>.
 37. La Russa MF, Comite V, Aly N, Barca D, Fermo P, Rovella N, Antonelli F, Tesser E, Aquino M, Ruffolo SA. Black crusts on Venetian built heritage, investigation on the impact of pollution sources on their composition. *Eur Phys J Plus*. 2018. <https://doi.org/10.1140/epjp/i2018-12230-8>.
 38. Zha J, Wei S, Wang C, Li Z, Cai Y, Ma Q. Weathering mechanism of red discolorations on Limestone object: a case study from Lingyan Temple Jinan, Shandong Province, China. *Herit Sci*. 2020;8:1–12. <https://doi.org/10.1186/s40494-020-00394-z>.
 39. Fassina V, Borsella B. The effects of past treatments on the acceleration of weathering processes in the statues on Prato della Valle. *Conserv Stone Other Mater*. 1993;1:129–36.
 40. Sabbioni C, Zappia G. Oxalate patinas on ancient monuments: the biological hypothesis. *Aerobiologia (Bologna)*. 1991;7:31–7.
 41. Benavente D, De Jongh M, Cañaveras JC. Minerals weathering processes and mechanisms caused by capillary waters and pigeon droppings on porous limestones. *Minerals*. 2020. <https://doi.org/10.3390/min>.
 42. Nimis P. *The Lichens of Italy. A second annotated catalogue*, EUT, 2016: pp. 739. ISBN 9788883037542
 43. Caneva G, Nugari MP, Salvadori O. *La biologia vegetale per i beni culturali*, Nardini, 2007: pp. 400. ISBN 9788840441535
 44. Dalla Costa M, Carbonara G, eds., *Memoria e Restauro dell'Architettura*. Saggi in onore di Salvatore Boscarino, Ex fabrica Franco Angeli, Milan, 2005: pp. 384. ISBN 8846469577
 45. Fassina V, Rossetti M, Fumo G, Zezza F, Macri F. The marble decay of Pilastrini Acritani and problems of conservation. In: Thiel MJ (Ed.), *Proceedings of the International RILEM/UNESCO Congress "Conservation of Stone and Other Materials: Research-Industry-Media"* Held at UNESCO Headquarters, Paris, June 29-July 1, 1993, ©RILEM, 1993: pp. 75–82.
 46. V. Fassina, M. Rossetti, H. Ott, F. Zezza. Weathering of marble in relation to natural and anthropogenic agents on the Ca' d'Oro facade (Venice). In: *Proceeding of the 3rd International Symposium on the Conservation of Monuments in the Mediterranean Basin*, Venice, 1994: pp. 825–834.
 47. Tesser E, Funghi meristemati su Pietra d'Istria: prove comparative di pulitura, Università Ca' Foscari, 2008.

Publisher's Note

Springer Nature remains neutral with regard to jurisdictional claims in published maps and institutional affiliations.

Submit your manuscript to a SpringerOpen® journal and benefit from:

- Convenient online submission
- Rigorous peer review
- Open access: articles freely available online
- High visibility within the field
- Retaining the copyright to your article

Submit your next manuscript at ► [springeropen.com](https://www.springeropen.com)